

# Reflection-enabled Directional MAC Protocol for Underwater Sensor Networks

Lloyd Emokpae and Mohamed Younis

Department of Computer Science and Electrical Engineering  
University of Maryland Baltimore County  
Baltimore, MD 21250  
{lemokpl,younis}@cs.umbc.edu

**Abstract**—Current medium access (MAC) protocols for underwater acoustic sensor networks (UW-ASNs) rely on omni-directional antennas as the basis for communication. The spatial inefficiency of such an antenna model limits the maximum achievable network throughput. This paper introduces a novel directional MAC protocol for UW-ASN that is based on a switch-beamed directional acoustic antenna and is not dependent on the line-of-sight (LOS). In the proposed reflection-enabled directional medium access (RED-MAC) protocol, each source node will be able to determine if an obstacle or another node is blocking the LOS link to the destination and switch to the best available directional antenna that will be reflected from the water surface or bottom. The destination will be able to determine if the received signal is the LOS or surface/bottom reflected by applying a homomorphic deconvolution process. The simulation results demonstrate the effectiveness of RED-MAC and the superiority of its performance in comparison to existing UW-ASN MAC protocols.

**Keywords**—underwater medium access protocol, directional MAC, underwater sensor networks

## I. INTRODUCTION

Underwater acoustic sensor networks (UW-ASNs) have applications in coastal protection, tactical surveillance and oceanic studies [1]. Although the propagation of acoustic signals is five orders of magnitude slower than the propagation of radio signals in air, it provides the best means of communication in water since radio waves are prone to high scattering and absorption in the water medium. However, the slow propagation of the acoustic medium complicates medium access arbitration [1][2]. MAC protocols for omni-directional antennas are either contention-based [3] or contention-free [4]. Contention-free protocols include time, frequency, and code division multiple access (TDMA, FDMA, and CDMA) schemes. While Contention-based protocols require each node to compete for the shared channel resulting in probabilistic coordination such as the carrier sense multiple access protocol (CSMA).

Time-based contention-free medium access is inefficient due to the need for a large guard time in order to cope with the worst case propagation delay. This would result in a waste of the limited acoustic channel bandwidth. Meanwhile, the narrow acoustic band makes FDMA-based medium access sharing impractical. Furthermore, it becomes hard to predict collisions among multiple node transmissions due to the

variant and slow propagation delay and thus contemporary CSMA protocols would not be able to solve the hidden terminal problem without some knowledge about the network topology.

Directional MAC (D-MAC) protocols usually surpass those based on omni transmissions in terms of bandwidth utilization and delay. Although D-MAC protocols have been studied extensively in RF environments, to date little attention has been given to acoustic links. This paper proposes a novel reflection-enabled directional MAC (RED-MAC) protocol, which to the best of our knowledge, is the first directional MAC for UW-ASNs that comprehensively addresses the various design complications of underwater medium access arbitration. The proposed RED-MAC protocol only requires one switch-beamed antenna which can be partitioned to form segmented directional antennas and will not be dependent on the line-of-sight (LOS) path. In traditional D-MAC protocols nodes can only direct their antennas towards the known position of the receiver. As a result, traditional D-MAC schemes cannot recover if an obstacle is blocking the path of the signal. However, with RED-MAC nodes will be able to determine if an obstacle is blocking the LOS link and switch to the next best directional antenna that will be reflected from the water surface or the water bottom. RED-MAC will achieve this by incorporating the surface-based reflection (SBR) scheme [5] which allows a receiver to establish water surface (or bottom) reflected links through a homomorphic deconvolution process. RED-MAC is validated through simulation experiments. The simulation results demonstrate that RED-MAC utilizes the acoustic channel very effectively and outperforms contemporary schemes.

The paper is organized as follows. In section II, we discuss related work in the literature. Section III goes over shallow water communication with SBR, while section IV goes over the directional acoustic antenna model. In section V, we present the proposed RED-MAC protocol. The validation results are presented in section VI. Section VII concludes the paper.

## II. RELATED WORK

As mentioned earlier both contention-based and contention-free protocols have been pursued for UW-ASNs. However, these protocols either are geared for saving energy [6] or focus on avoiding the effect of propagation delay on access collisions [3] without much care for bandwidth utilization.

Meanwhile CDMA-based approaches [4] do not work well in shallow water environments. Some protocols have pursued hybrid schemes such the clustered-network architecture in [7], where nodes are grouped based on proximity. TDMA is used within the individual clusters since the distance between nodes is small and the guard time between time slots does not have to be large. Interference among clusters is prevented by allocating distinct spreading code to each cluster. Meanwhile, the Slotted-FAMA protocol [8] combines TDMA and CSMA in order to achieve high throughput. However, the involved handshaking may lead to low throughput in the presence of high propagation delay in the underwater acoustic channel. In addition, the protocol requires clock synchronization, which is very challenging to achieve in UW-ASNs due to the slow signal propagation. An extension has been proposed in [9] to eliminate the need for clock synchronization by adjusting the handshake time based on the distance between the communicating nodes.

R-MAC [10] strives to save energy and avoid collisions through medium access reservation. A node randomly picks its listening/sleep and transmission schedule and informs its neighbor. However, the protocol only works well as long as the network topology (i.e. neighborhood) is known and remains static. R-MAC protocol also does not take into account the large propagation delays in the UW-ASNs that may affect the transmission. Meanwhile, in Tone-LoHi (T-Lohi) [11] nodes contend to reserve the channel for the right to transmit data. Nodes will contend for access to the channel by sending a short tone and listening for a tone from other contenders to determine if the reservation was successful. The T-Lohi protocol takes into account the slow underwater signal propagation by adjusting the reservation period based on the expected propagation delay. Despite the major improvement in channel throughput and energy savings, there are still some cases of data-to-data collisions due to bi-directional deafness. T-Lohi also does not have a mechanism for detecting a hidden terminal. Furthermore, T-Lohi is based on omni-directional transmission and does not take full advantage of the available spatial spectrum.

Directional MAC protocols usually surpass those based on omni transmissions in terms of bandwidth utilization and delay. Although directional MAC (D-MAC) protocols have been studied extensively in RF environments, to date no protocol exists for UW-ASNs. Therefore, we cover some of the RF-based D-MAC protocols that may be applied to UW-ASNs. In [12], a node uses two antennas for communication, one directional used for sending and one omni-directional dedicated for receiving. In the DtD-MAC protocol [13], each node will use a low-cost switch-beamed antenna for both transmission and reception. A transmitter continually scans the directional antenna towards the known receiver and sends a D-RTS message when the antenna is not blocked. If the receiver's position is not known the transmitter will sequentially send D-RTS messages on each of the unblocked antenna and then waits for a reply before continuing clockwise to the next antenna. A receiver will periodically scan each of its directional antennas for D-RTS messages by waiting for a

specified amount of time (on each antenna) before switching counter-clockwise to the next antenna. This leads to increased delivery delay and would not thus be suitable for mediums that has the slow signal propagation.

### III. SHALLOW WATER COMMUNICATION WITH SBR

In this section, we will go over shallow water communication with reflected links (i.e. SBR). We will start by first deriving expressions for the transmission loss in the shallow water environment (part A) which will be used in the filtering process required by SBR to utilize reflected links (part B). It is assumed that each node will be aware of its position and that of its neighbors by applying suitable localization techniques such as [18].

#### A. Acoustic Transmission Loss

As mentioned earlier, the slow propagation delay in the underwater channel makes medium arbitration a challenge. According to [14] the sound speed ( $c$ ) is dependent on the temperature ( $T$ ) in degrees centigrade, salinity ( $S$ ) in parts per thousand, and depth ( $z$ ) in meters. This can be expressed mathematically as shown:

$$c = 1449.2 + 4.6T - 0.055T^2 + 0.00029T^3 + (1.34 - 0.01T)(S - 35) + 0.016z \quad (1)$$

We can further simplify the expression in (1) for shallow water environments and assume a sound speed profile that varies pseudo-linearly with depth as introduced by Gordon [17]:

$$c(z) = \frac{c_w}{\sqrt{1+2.4z/c_w}} \quad (2)$$

where,  $c_w$  is the speed of sound close to the water surface and  $z$  is the node's depth in the shallow water environment. In RED-MAC we refer to the average sound speed between to connecting nodes  $i$  and  $j$  with depths ( $z_i, z_j$ ) as:

$$\bar{c}_{ij} = (c(z_i) + c(z_j))/2 \quad (3)$$

In general, there are three main causes of transmission loss in an underwater environment which are transmission loss due to multipath attenuation effects ( $TL_{MULT}$ ), transmission loss due to spherical geometric spreading ( $TL_{SGP}$ ) and transmission loss due to plane-wave attenuation, i.e. absorption ( $TL_{WAVE}$ ) [14]. The total transmission loss in decibels can be expressed mathematically as:

$$TL_{TOTAL} = TL_{MULT} + (TL_{SGP} + TL_{WAVE})$$

$$TL_{TOTAL} = TL_{MULT} + TL_{LOS} \quad [dB] \quad (4)$$

where we have now grouped the spherical geometric spreading  $TL_{SGP}$  and plane-wave  $TL_{WAVE}$  transmission loss to what we define as the line-of-sight (LOS) transmission loss  $TL_{LOS}$ . In shallow water most of the transmission loss is due to the attenuation from multipath effects. The total signal attenuation  $\alpha_{TOTAL}$  can then be expressed as:

$$\alpha_{TOTAL} = \frac{1}{1000} \left( \frac{TL_{MULT}}{\lambda} + \frac{TL_{LOS}}{k_{LOS}} \right) \quad [dB/km]$$

$$\alpha_{TOTAL} = \alpha_{MULT} + \alpha_{LOS} \quad [dB/km] \quad (5)$$

Such that  $\lambda$  is the acoustic signal wavelength in meters and  $k_{LOS}$  is the LOS transmission range (also in meters). The LOS transmission loss  $TL_{LOS}$  (in dB) has the following frequency-distance  $d$  (in meters) dependent relationship:

$$TL_{LOS} = 2 \cdot 10 \log(d) + \tilde{\alpha}(f)d \quad [dB] \quad (6)$$

where  $\tilde{\alpha}(f)$  is the attenuation due to absorption and  $f$  is the frequency in kHz. The multipath transmission loss  $TL_{MULT}$  can be determined by modeling the shallow water environment as a homogeneous fluid-fluid media as illustrated in Figure 1(a). The top layer is the water layer and the bottom layer is the oceanic bottom in a shallow water environment. In the water layer the parameters  $\{c_w, p_w, \theta_w\}$  correspond to the speed of sound (in m/s), the density (in kg/m<sup>3</sup>) and grazing angles (in radians). The same applies for the parameters  $\{c_b, p_b, \theta_b\}$  in sea bottom. The multipath transmission  $TL_{MULT}$  can then be estimated by calculating the Raleigh reflection coefficients (using Snell's Law) as shown:

$$R = \frac{p_b c_b / \sin \theta_b - p_w c_w / \sin \theta_w}{p_b c_b / \sin \theta_b + p_w c_w / \sin \theta_w}$$

$$\hat{R}_{bottom}(\theta) = R e^{-0.5\Gamma^2} \quad (7)$$

$$\hat{R}_{water}(\theta) = -e^{-0.5\Gamma^2} \quad (8)$$

$$TL_{MULT} = \begin{cases} -10 \log(|\hat{R}_{water}(\theta)|^2) & \text{Water} \\ -10 \log(|\hat{R}_{bottom}(\theta)|^2) & \text{Bottom} \end{cases} \quad (9)$$

where  $R$  is the reflection coefficient for a flat bottom and  $\Gamma = 2k\sigma_{RMS} \sin \theta$ . The Raleigh roughness parameter  $\Gamma$  depends on the wavenumber  $k = 2\pi/\lambda$ , the root-mean-square (RMS) roughness  $\sigma_{RMS}$  and the grazing angle  $\theta = \theta_w$ . We can further derive attenuation factors ( $\alpha_b$  and  $\alpha_w$ ) for the water surface and bottom as shown:

$$\alpha_b = \frac{1}{1000} \left( \frac{-10 \log(|\hat{R}_{bottom}(\theta)|^2)}{\lambda} \right) [dB/km] \quad (10)$$

$$\alpha_w = \frac{1}{1000} \left( \frac{-10 \log(|\hat{R}_{water}(\theta)|^2)}{\lambda} \right) [dB/km] \quad (11)$$

The bottom attenuation can also be measured for different bottom materials (i.e. silt, gravel, basalt, etc). The impact of the multipath transmission loss  $TL_{MULT}$  for different grazing angles is shown in Figure 1(b), where we see the effect of high grazing angles  $\theta = \theta_w$  on the transmission loss.

### B. Surface-based Reflection Overview

To establish reflected links we incorporate SBR which inherits the ray propagation model for modeling signal

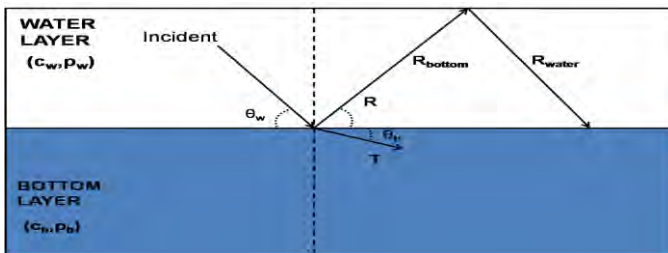


**Figure 1(a):** Illustration of a fluid-fluid medium used to calculate the reflection coefficients. (R, T) are the reflected and transmitted coefficients respectively.

propagation in shallow water. With SBR, there are three types of eigenrays (traveling wave) that are of interest namely: direct-path (DP) or LOS, refracted-surface-reflected (RSR), and refracted-bottom-reflected (RBR). SBR then models the acoustic channel as a multi-path channel where the received signal  $r(t)$  at the receiver can be determined by convolving the transmitted signal  $e(t)$  with the channel's impulse response (IR)  $h(t)$  as shown:

$$r(t) = s(t) + n(t) = e(t) * h(t) + n(t)$$

$$r(t) = \sum_{k=1}^K \beta_k e(t - \tau_k) + n(t)$$

The values of  $\beta_k$  and  $\tau_k$  correspond to the attenuation factor and the time delay for the  $k$ -th path,  $s(t)$  and  $n(t)$  correspond to the noise-free signal and additive noise respectively. The time delay can be determined by the geometry information of the transmitter and receiver pairs with depths  $\{D_{TX}, D_{RX}\}$ , water depth  $D_w$  and LOS distance  $d$  as shown:

$$\tau_i = \frac{r_k}{c_{ij}} = \frac{\sqrt{(D_{TX} + a_k D_w + b_k D_{RX})^2 + d^2}}{c_{ij}} \quad (12)$$

For an eigenray length of  $r_k$  that is dependent on the average sound speed between the two connected nodes  $c_{ij}$  as defined in (3). Each eigenray length  $r_k$  is reflected at the surface first before being reflected  $k$  times during the entire propagation. The coefficients  $a_k$  and  $b_k$  are expressed as,  $a_{k+1} = a_k + (1 + (-1)^{k+1})$ ; for  $a_1 = 0$  and  $b_k = (-1)^{k+1}$ . SBR then recovers both the LOS and the reflected signals by first calculating the attenuation due to multipath from the recovered IR namely  $h_r[n]$ , where  $h_r[n] \cong h[n] = h(nf_s^{-1})$  for a sampling frequency of  $f_s$  in Hz. To do this, we define a new parameter  $\alpha_{h_r}$  which is the attenuation from the recovered channel IR  $h_r[n]$  and is defined as follows:

$$\alpha_{h_r} = \frac{1}{1000} \left( \frac{-10 \log(|H(z)|)}{\lambda} \right) [dB/km] \quad (13)$$

where,  $H(z)$  is the frequency response of the recovered channel IR for  $z = e^{jw}$  and  $w = 2\pi f_s$ . To determine if the attenuated signal was reflected from the water surface, we apply the mathematical condition expressed in (14) and select option II to recover the RSR eigenray. Where the attenuation parameters ( $\alpha_{LOS}, \alpha_w, \alpha_b$ ) and are known from the previous subsection.

$$\begin{cases} (I) & \alpha_{h_r} \leq \alpha_{LOS} & \text{LOS} \\ (II) & \alpha_{LOS} < \alpha_{h_r} \leq \alpha_{LOS} + \alpha_w & \text{RSR} \\ (III) & \alpha_{LOS} + \alpha_w < \alpha_{h_r} \leq \alpha_{LOS} + \alpha_b & \text{RBR} \end{cases} \quad (14)$$

The expression (14) implies that  $\alpha_b > \alpha_w$  which is common in underwater acoustics. A detailed manuscript of the SBR recovery process (i.e. recovery of  $h_r[n]$ ) can be found in [5].

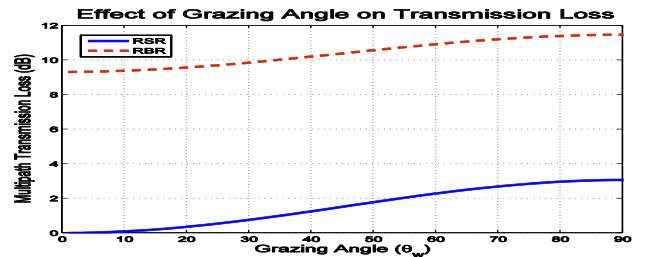


**Figure 1(b):** Multipath transmission loss for a silt-like rough bottom and a rough water surface with rms roughness of 0.1

#### IV. ACOUSTIC ANTENNA MODEL

In order to mitigate the multipath effects described in the previous section, our RED-MAC protocol will utilize directional acoustic antennas. A directional underwater acoustic antenna is composed of an array of hydrophones that can be summed up at various phases and amplitudes resulting in a beam-former [14]. An omni-directional beam-former can be expressed by averaging the signal-to-noise ratio (SNR) to the output of the hydrophone array as follows:

$$SNR = \frac{S^2}{N^2} = \frac{[\sum_{i=1}^m s_i(t)]^2}{[\sum_{i=1}^m n_i(t)]^2} = \frac{\sum_{i=1}^m \sum_{j=1}^m s_{ij}}{\sum_{i=1}^m \sum_{j=1}^m n_{ij}} \quad (15)$$

where the bar represents the average over time of the  $m$  signals  $s_i(t)$  and noise  $n_i(t)$ . The array signals and noise for the  $i^{\text{th}}$  and  $j^{\text{th}}$  hydrophones can be expressed as  $s_{ij} = s^2 \hat{s}_{ij}$  and  $n_{ij} = n^2 \hat{n}_{ij}$ . Thus, the beam-former can be further simplified to:

$$\frac{S^2}{N^2} = \frac{s^2 \sum_{i=1}^m \sum_{j=1}^m \hat{s}_{ij}}{n^2 \sum_{i=1}^m \sum_{j=1}^m \hat{n}_{ij}}$$

The gain of the hydrophone array can then be expressed as:

$$AG = 10 \log \left( \frac{S^2}{N^2} \right) = 10 \log \left( \frac{\sum_{i=1}^m \sum_{j=1}^m \hat{s}_{ij}}{\sum_{i=1}^m \sum_{j=1}^m \hat{n}_{ij}} \right)$$

In the design of RED-MAC, we will need to know the maximum number of directional antennas available which we define as  $\Lambda = m$ , where  $m$  is the number of available directional antennas. It is also common to know the beam steering angle  $\theta = \theta_s$ , which is also referred to as the look direction. A vector hydrophone array was developed in [15] for underwater acoustic communication. Figure 2 shows an illustration of the 7-element 3D vector sensor array with sensors oriented at both positive and negative axis  $\pm (x, y, z)$  as well as at the origin  $(0,0,0)$ . When combined together, the 7 elements can be used as an omni-directional antenna with beam pattern shown in the right side of Figure 2 (the dipole is the omni-directional beam oriented around the x-axis). Each antenna processing element will then apply the SBR multipath filtering process (section III) when enabled by the RED-MAC protocol.

#### V. REFLECTION-ENABLED DIRECTIONAL MAC PROTOCOL

RED-MAC is broken up into two phases namely, (i) node discovery, and (ii) directional antenna allocation (DAA) for data transfer. In node discovery, each node will use the water surface (or bottom) to locate its one-hop neighbors; this is accomplished by using a tone-induced directional carrier sensing protocol. The purpose of the DAA phase is to allocate the directional antenna for data transfers by considering both LOS and reflected (SBR) paths in an integrated manner. A

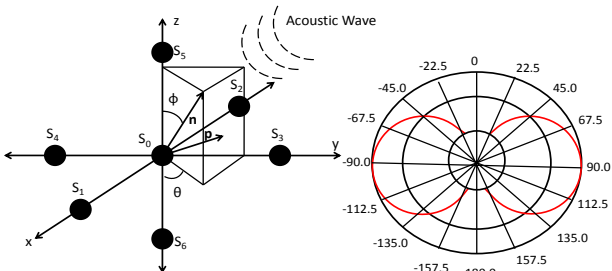


Figure 2: A 7-element antenna array [15] and the corresponding beam-form pattern when combining the signals oriented around the x-axis.

high level overview of the RED-MAC transmitter operation is shown in Figure 3 (the state diagram for the receiver is omitted due to space constraints).

##### A. Node Discovery Phase

To access the medium during this phase, each node will adhere to the following tone-induced directional carrier sensing protocol. The protocol starts by requiring each node to sense each directional antenna before sending tone-discovery (TD) messages to locate its one-hop neighbors. The right block in Figure 3 describes the transmitter operation during the node discovery phase. A node will start by sensing the sectors of the antenna (those pointing towards the water surface) for a period of  $t_{SENSE} = 2 * t_{max}$ , where  $t_{max} = k_{LOS}/c_w$  is the maximum one-way propagation delay between any two nodes within the specified transmission range  $k_{LOS}$ . Within the  $t_{SENSE}$  period, if the node detects another tone or a data transfer on the specified directional antenna, the node will mark that antenna as blocked for a period of  $t_{DATA}(d_i)$ . The transmitter will then perform an active node discovery by sending TD pings on each of the free directional antennas, and listening for a tone-ack (TA) on each of the directional antennas directed towards the water surface (or water bottom).

Due to the multipath nature of the underwater environment, the node will need to filter out all other signals that are reflected multiple times as demonstrated in (14). Following the TA message, there will be the data payload which will contain the position, the movement direction, and the movement speed of the receiver on that directional antenna ( $d_i$ ). The transmitter will use this information to change its antenna based on the movement of the receiver.

After the transmitter has received a TA message on any of its directional antennas, the node will then complete node discovery and will move to the directional antenna allocation (DAA) phase for data transfer. Upon acknowledging the discovery tone, the receiver switches to the data transfer phase. The receiver also maintains a Directional Network Allocation Vector (DNAV) table which contains information about the clear-to-send (CTS) and data transmission time of each directional antenna, the usage of the DNAV table is common in directional MAC protocols [12][13].

##### B. Directional Antenna Allocation (DAA) For Data Transfer

After a node has discovered its one-hop neighbors, the next step will be to determine the best way to allocate its directional antennas to fully utilize the available spatial spectrum. The left block in Figure 3 describes the DAA phase of RED-MAC. If a transmitter has data to send to a known receiver, it will re-calculate the estimated position of the

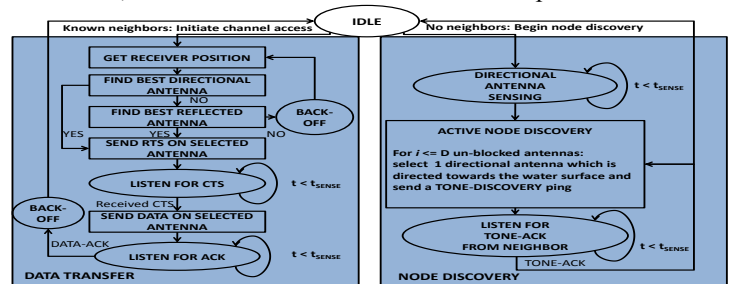


Figure 3: RED-MAC transmitter state diagram



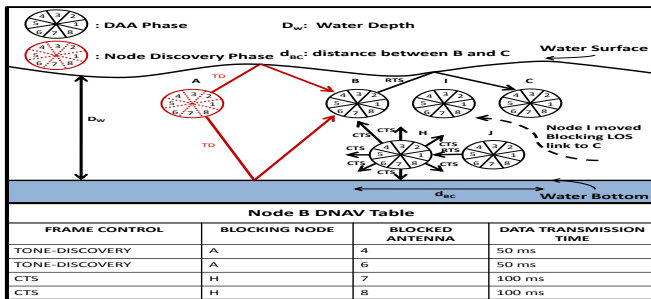
receiver if the receiver is mobile; otherwise it will simply use the last known position. The transmitter will then sense the antenna that is directed towards the receiver to see if it is blocked. This done by checking the DNAV table which contains the heard CTS and TD messages ongoing on the blocked antennas. The receiver will respond to RTS by sending CTS on all available antennas, i.e., those which do not interfere with ongoing communications.

Figure 4 illustrates a 2D scenario whereby the node  $B$  wants to send data to the node  $C$ . Nodes  $B$ ,  $C$ ,  $I$ ,  $H$  and  $J$  are already discovered and node  $A$  tries to join the network by sending a discovery tone to  $B$ . Within the same period, nodes  $J$  and  $H$  undergo a data transfer handshaking process, where node  $J$  sends RTS to the known node  $H$  and node  $H$  will send a CTS on all un-blocked directional antennas. Since node  $I$  moved and blocked the LOS path between nodes  $B$  and  $C$ , for transmitter  $B$  the next best directional antenna to  $C$  can only be antenna 2 (since antenna 8 is also blocked), which is the antenna that will reflect unto the water surface. The transmitter  $B$  will be able to determine that the node  $I$  is blocking its path since it knows the movement direction and speed of node  $I$ . After the transmitter selects the best directional antenna (in this example antenna 2 will reflect unto node  $C$ ), it sends the RTS on that antenna and waits for  $t_{SENSE} = 2 * t_{ij} = 2 * r_{ij} / \bar{c}_{ij}$  period to receive the CTS message from node  $C$  in order to send the data. The surface-reflected distance  $r_{ij}$  is derived from (12), while the distance  $d_{ij}$  is the LOS distance between the nodes  $i$  and  $j$  (i.e.  $d_{BC}$ ) with depths  $\{z_i, z_j\}$ . The average sound speed  $\bar{c}_{ij}$  between the two nodes is defined in (3). RED-MAC also employs back-off mechanism (see Figure 3) after each successful data transfer to promote fairness on the acoustic channel.

RED-MAC has many advantages. First, it strives to maximize spatial efficiency of underwater medium by considering both reflected and LOS paths in an integrated manner when allocating the directional antennas. Second, it alleviates the hidden terminal problem that is common in directional MAC protocols since TD and the CTS messages are sent using all available directional antennas. Third, RED-MAC leverages the node's knowledge about the motion pattern of neighbors and enables the rediscovery of a node that loses LOS link due to unexpected motion or drift.

## VI. RED-MAC EVALUATION

In this section we will validate the performance of the RED-MAC protocol and compare it to traditional UWMAC



**Figure 4:** A 2-dimensional example that demonstrates both phases of the proposed RED-MAC protocol. Node  $B$  wants to send data to node  $C$  while  $A$  tries to discover its neighbors, DNAV is shown for node  $B$ .

protocols. We have adopted the network simulator of [11] to study the performance of RED-MAC and added support for both directional and omni-directional antennas. STLoHi [11] and slotted-ALOHA (SALOHA) are used as baseline for comparison. In the simulation only RED-MAC utilizes the directional antenna model while the baseline protocols use omni-directional antennas. The simulation parameters are described in Table 1, where the depth-dependent sound speed for each node is computed from (2). Each RED-MAC node will utilize directional antennas with the option of enabling reflections (SBR). The network traffic is controlled by adjusting the network load (packets/sec). The mobility is controlled by adjusting the node speed (m/s) such that nodes with even and odd IDs will move in the  $x$  and  $y$  directions respectively. We randomly place  $N$  nodes in a  $300 \times 400$  area (water depth of 300 m) with a flat water surface and bottom. Each node randomly selects a unique destination out of the  $N-1$  remaining nodes. We then run each simulation for 100 seconds and repeat it 300 times to study the effects of varying the simulation parameters ( $N$ , node speed, network load) on the network throughput. Finally, we report the results where we observe that within a 95% confidence level the network throughput (bits/sec) stays within 5% of the sample mean.

### A. Network Throughput: Under Varying Network Density

In this subsection we study the effects of increasing the network density ( $N$ ) on the network throughput. Figure 5 shows a plot of the network throughput for four protocols (RED-MAC-no-SBR, RED-MAC-SBR, STLoHi, and SALOHA), both STLoHi and slotted-ALOHA are reservation-based protocols. From the plot we see that even without enabling reflections RED-MAC outperforms the other protocols as the network density increases by achieving up to 46% increase in throughput. This is due to the increase in the number of transmissions and successful receptions achieved in RED-MAC. With SBR we notice an additional 10% increase in throughput, since nodes can now utilize reflected links when the LOS links are blocked. We also notice that RED-MAC saturates around a network density of fourteen nodes, yielding a throughput of 1600 bps when SBR is employed, SALOHA saturates at 17 nodes while STLoHi saturates much quicker right around 2 nodes, this is due to the conservative scheduling nature of STLoHi. With SBR, RED-MAC achieves up to 56% increase in network throughput over both reservation-based protocols, since both STLoHi and SALOHA saturate to a throughput of 650 bps.

### B. Network Throughput: Under Varying Network Mobility

Figure 6 shows a plot that varies the node speed when some

$k_{LOS}$	$\theta_s$	Packet Length	Modem Rate
500m	45°	650 bytes	1 kb/s
$p_w$	$p_b$	$c_w$	$\Lambda$
998 kg/m <sup>3</sup>	1000 kg/m <sup>3</sup>	1510 m/s	8

$k_{LOS}$  : The line-of-sight (LOS) transmission range  
 $\theta_s$  : The beam steering angle  
 $p_w$  : Density in the water surface layer  
 $p_b$  : Density in the water bottom layer  
 $c_w$  : Sound speed in the water layer  
 $\Lambda$  : Number of directional antennas

**Table 1:** Simulation parameters

of the nodes in the network are mobile for a network density of  $N=20$  nodes. We see that for low mobility the network throughput remains stable when the number of mobile nodes is low with a slight increase for higher mobile nodes; this is because the transmitting node will try to maintain a connection with the mobile receiver by utilizing both reflected and LOS links. From the same plot, we see that as we increase the number of mobile nodes the network throughput increases, this is mainly due to the decrease in the number of collisions achieved by the increased node mobility. Therefore, we see that RED-MAC maintains a stable throughput performance for moderate node speeds (i.e. drifts). However, at high node speeds the throughput becomes less stable due to packet loss.

### C. Network Throughput: Under Varying Network Load

In this section we study the effect of varying the mean network load on the network throughput, for a network density of  $N=20$  nodes. Figure 7 shows that as we increase the mean network load the network throughput remains stable for each protocol. Most importantly we notice up to a 56% increase in throughput that RED-MAC achieves over traditional omni-directional UW-ASN MAC protocols.

## VII. CONCLUSION

In this paper we have introduced a novel directional medium access protocol for UW-ASN that is not dependent on the line-of-sight (LOS). The proposed reflection-enabled directional MAC protocol utilizes a switch-beamed directional antenna and employs a surface-based reflection (SBR) recovery mechanism; the transmitter will be able to recover if an obstacle is blocking the LOS path by applying a SBR filtering process to utilize reflected communication links to the receiver. The simulation results demonstrate the effectiveness of the RED-MAC protocol which achieves up to 56% increase in throughput in comparison to traditional omni-directional MAC protocols. The results also depict a stable network throughput for low to moderate network mobility. Hence RED-MAC provides a spatial efficient and mobility tolerant medium access arbitration for underwater sensor networks.

## ACKNOWLEDGEMENTS

This work was supported by the National Science Foundation (NSF) award # CNS 1018171.

## REFERENCES

[1] L. Liu, S. Zhou, and J.-H. Cui, "Prospects and Problems of Wireless Communications for Underwater Sensor Networks," *Wireless Communications and Mobile Computing*, Special Issue on Underwater Sensor Networks, Vol. 8, No. 8, pp. 977-994, May 2008.

[2] I. F. Akyildiz, D. Pompili, and T. Melodia, "Underwater Acoustic Sensor Networks: Research Challenges," *Ad Hoc Networks*, 3 (3), pp. 257-279, March 2005.

[3] X. Guo, M. R. Frater, and M. J. Ryan, "A Propagation-delay-tolerant Collision Avoidance Protocol for Underwater Acoustic Sensor Networks," *Proc of the MTS/IEEE Conf. and Exhibition for Ocean Engineering, Science and Tech. (OCEANS'06)*, Boston, MA, Sept 2006.

[4] D. Pompili, T. Melodia, and I. F. Akyildiz, "A CDMA-based Medium Access Control Protocol for Underwater Acoustic Sensor Networks," *IEEE Transactions on Wireless Communications*, vol. 8, no. 4, pp. 1899-1909, April 2009.

[5] L. Emokpae, M. Younis, "Surface Based Underwater Communications", *Proc. of the IEEE Global Communications Conf. (GLOBECOM'10)*, Miami, FL, December 2010.

[6] V. Rodoplu and M. K. Park, "An Energy-efficient MAC Protocol for Underwater Wireless Acoustic Networks," in the *Proceedings of the MTS/IEEE Conference and Exhibition for Ocean Engineering, Science and Technology (OCEANS'05)*, Washington, DC, September 2005.

[7] F. Salva-Garau and M. Stojanovic, "Multi-cluster Protocol for Ad-Hoc Mobile Underwater Acoustic Networks," in the *Proceedings of the MTS/IEEE Conference and Exhibition for Ocean Engineering, Science and Technology (OCEANS'03)*, San Francisco, CA, September 2003.

[8] M. Molins and M. Stojanovic, "Slotted FAMA: A MAC Protocol for Underwater Acoustic Networks," in the *Proceedings of MTS/IEEE OCEANS'06 Conference*, Boston, MA, September 2006.

[9] B. Peleato and M. Stojanovic, "A MAC Protocol for Ad-Hoc Underwater Acoustic Sensor Networks," in the *Proceedings of the 2<sup>nd</sup> ACM International Workshop on Underwater Networks (WUWNet'07)*, Montreal, Quebec, Canada, September 2007.

[10] P. Xie and J.H. Cui, "R-MAC: An Energy-Efficient MAC Protocol for Underwater Sensor Networks," in the *Proceedings of IEEE International Conference on Wireless Algorithms, Systems and Applications (WASA'07)*, Chicago, IL, August 2007.

[11] A. Syed, W. Ye, and J. Heidemann, "T-Lohi: A New Class of MAC Protocols for Underwater Acoustic Sensor Networks," in the *Proceedings of IEEE INFOCOM 2008*, Phoenix, AZ, April 2008.

[12] R. Ramanathan, J. Redi, C. Santivanez, D. Wiggins, S. Polit, "Ad Hoc Networking with Directional Antennas: A Complete System Solution," *IEEE Journal on Selected Areas in Communication*, Vol. 23, No. 3, pp. 496-506, March 2005.

[13] E. Shihab, C. Lin, P. Jianping, "A Distributed Asynchronous Directional-to-Directional MAC Protocol for Wireless Ad Hoc Networks," *IEEE Transactions on Vehicular Technology*, Vol. 58, No. 9, pp. 5124-5134, November 2009.

[14] F.B. Jensen, W.A. Kuperman, M.B. Porter, H. Schmidt, *Computational Ocean Acoustics*, Springer New York, 2<sup>nd</sup> edition.

[15] N. Zou, C.C. Swee, B.A.L. Chew, "A Vector Hydrophone Array Development and its Associated DOA Estimation Algorithms," in the *Proceedings of OCEANS Asia Pacific*, pp. 1-5, Singapore, May 2006.

[16] D. Chizhik, A.P. Rosenberg, Q. Zhang, "Coherent and Differential Acoustic Communication in Shallow Water Using Transmitter and Receiver Arrays," in the *Proceedings of IEEE OCEANS (OCEANS'10-Sydney)*, pp. 1-5, Sydney, Australia, May 2010.

[17] M.A. Pedersen and D.F. Gordon, "Normal-mode and ray theory applied to underwater acoustic conditions of extreme downward refraction," *J. Acoust. Soc. Am.* 51, 323-368 (1972)

[18] A. Youssef, M. Younis, M. Youssef and A. Agrawala, "On the Accuracy of Multi-hop Relative Localization Estimation in Wireless Sensor Networks", Submitted for publication, 2006

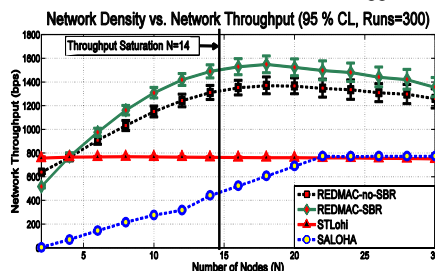


**Figure 5:** A higher network density boosts the throughput achieved by RED-MAC, since multiple transmissions can occur within the same communication range.

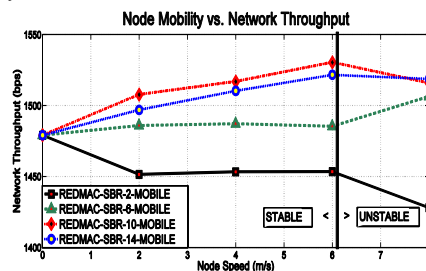


**Figure 6:** We see a stable throughput performance for low network mobility, however higher network mobility leads to packet loss.

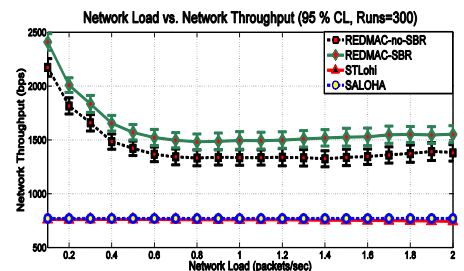


**Figure 7:** While each studied MAC protocol maintains a steady throughput as the mean packet load increases, RED-MAC outperforms traditional UWMAC protocols by up to 56%.